

Radiation Dose and Image Quality in Various Examinations and Imaging Modes of Dentomaxillofacial Cone Beam Computed Tomography

Mohammad Taghi Bahreyni Toossi¹, Navid Zafari¹, Seyed Hosein Hoseini-Zarch², Elham Dolat¹, Hosein Azimian¹, Majid Sadeghi Moghadam^{1*}

1. Medical Physics Research Center, Mashhad University of Medical Sciences, Mashhad, Iran.
2. Department of Oral and Maxillofacial Radiology, School of Dentistry, Mashhad University of Medical Sciences, Mashhad, Iran.

ARTICLE INFO	ABSTRACT
Article type: Original Paper	Introduction: Cone-beam computed tomography is used for specialized imaging of dental and maxillofacial structures. CBCTs capabilities and facilities for dental and maxillofacial imaging have resulted in their increasing clinical use. Although the dose of CBCT tests is low, its widespread use increases the cumulative dose. This study was conducted to evaluate head and neck effective dose and image quality in different organs for various exposure techniques in CBCT imaging.
Article history: Received: Feb 28, 2021 Accepted: Jun 03, 2021	Material and Methods: This study was performed on various CBCT imaging examinations. Head and neck parts of anthropomorphic male Rando® Alderson Phantom and thermoluminescent dosimeters were used for organ dosimetry. Contrast to noise ratio and signal to noise ratio were evaluated for image quality assessments. For this purpose, the region of the tooth and soft tissue images were randomly used as the basis.
Keywords: Radiation Dose Maxillofacial Cone Beam Computed Tomography Dental Imaging Signal To Noise Ratio	Results: Mean effective dose for face and paranasal sinuses imaging in three modes (standard, low-dose, ultra-low dose), temporomandibular imaging in two modes (standard & low dose), and dental imaging in implant and endo imaging modes was equal to 382.17, 193.97, 79.96, 262.6, 135.67, 53.93, 682.83, 335.75, 184.18, and 234.57 μ Sv, respectively. Signal -to -noise ratio (SNR) for the above-mentioned procedures was equal to 6.04, 5.73, 3.71, 6.3, 6.00, 4.08, 14.2, 12.3, 7.51, and 6.97, respectively. Conclusion: The present study showed, when low dose and ultra-low-dose modes are chosen, the patient's dose will be severely reduced in most CBCT procedures. Contrast-to-noise ratio (CNR) and SNR will diminish too, but they are sufficient for some diagnostic purposes.

► Please cite this article as:

Bahreyni Toossi MT, Zafari N, Hoseini-Zarch H, Dolat E, Azimian H, Sadeghi Moghadam M. Radiation Dose and Image Quality in Various Examinations and Imaging Modes of Dentomaxillofacial Cone Beam Computed Tomography. Iran J Med Phys 2022; 19: 159-166. 10.22038/IJMP.2021.56040.1932.

Introduction

Cone-beam computed tomography (CBCT) is a method used for the specialized imaging of dental and maxillofacial structures. In this method, X-ray tube rotates around the patient's head partially or completely. A cone shape X-ray beam and a 2D flat detector produce a series of 2D images[1]. These data are applied for the reconstruction of various 3D anatomical images as well as the reformation of sagittal, axial, and coronal planes [2, 3].

CBCT imager equipment can create images with high spatial resolution, lower radiation dose, and lesser cost in comparison with conventional computed tomography (CT). They have more capabilities and facilities for dental and maxillofacial imaging[4, 5].

Although the periapical 2D film is commonly used for dental lesions, CBCT has a higher priority for diagnosing dental and periodontal lesions. Given the variety of CBCT systems' capabilities, the demand for their application is constantly increasing[3, 6].

CBCT systems are applied for imaging in oral and maxillofacial surgery, implantology, temporomandibular joint (TMJ) disorders, orthodontics, endodontics, orbital and nasal skeletal assessment, and pre-and post-surgery evaluations of paranasal sinuses [2, 7-9].

Effective radiation dose in CBCT is lower than conventional computed tomography(CT) and multi-slice CT (MSCT) systems[10, 11]. Although the radiation dose in the CBCT system is somewhat low, cumulative dose should also be considered due to the increase in the use of CBCT. Also, the effective dose is variable between CBCT units[12].

Most CBCT units have various protocols and exposure settings for imaging different anatomic regions. Thus, effective dose level and image quality parameters vary concerning the selection of the imaging techniques. In this regard, the selection of the optimized technique is necessary for minimizing the

patient's radiation dose while obtaining images with sufficient diagnostic quality[13, 14]. This is very important for all patients, especially infants, as well as pregnant women.

For this reason, in the current survey, organ dose and image quality parameters were assessed for various CBCT imaging and exposure settings.

Materials and Methods

CBCT Scanner

Planmeca ProMax® 3D Max CBCT unit (Helsinki, Finland) was used for imaging. Some of the features of this CBCT unit are: tube voltage of 60–120 kV, anode current of 1–12 mA, focal spot of 0.6 mm, with a fixed anode, image detector: flat panel, single image acquisition with 210 / 360 degrees of rotation, scan time of 9–55 s and typical reconstruction time of 2–25 s. Various imaging protocols were predefined for each anatomic area, although radiographers can change most exposure settings for better outcomes depending on the patient's anatomy and imaging area.

In this study, effective doses were evaluated for the most common radiological tests in dental and maxillofacial examinations, through the CBCT unit. Radiologic examinations and their exposure setting are presented in the following table.

Dosimeter

Thermoluminescent dosimeters 100 (TLD100 Harshaw Chemical Company, OH, USA) were applied in this survey. TLD100 consisting of LiF:Mg,Ti can detect the dose level as low as $\sim 10 \mu\text{sv}$. For calibration of TLDs, an ionizing chamber Radcal® dosimeter model 9015 (Radcal Corporation, Monrovia, California, USA) was applied. TLDs and the ionizing chamber were exposed to radiation three times, in similar geometric and diagnostic X-ray energy, then average conversion coefficients were obtained. The TLDs were placed in the desired anatomical areas of the phantom. Figure 1 shows the TLD placement for lens dosimetry.

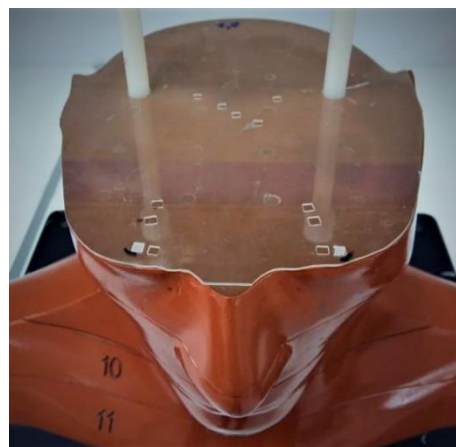


Figure1. TLDs Placement in desired anatomical areas.

For organ dose measurement, TLDs were inserted for right and left thyroid lobes, right and left parotid and salivary glands, right and left lens of eyes, and neck soft tissue concerning their anatomical location in the phantom under the guidance of radiologist.

TLDs were annealed in a two-step process, 400 °C for 1 hour and 100 °C for 2 hours. Five non-irradiated TLDs were used for background dosimetry and this dose was deducted from the dose measured for organs. After examination, thermoluminescent dosimeters were read by Harshaw 3500 TLD reader (USA).

For measuring organs dose, in each exposure technique, irradiation was performed three times and the averaged TLD Values were calculated.

Phantom

For the estimation of the effective dose, an anthropomorphic phantom can be used [15, 16]. So Anthropomorphic male Rando® Alderson Phantom (Rando Alderson Research Laboratories, NY, USA) was used in this study. This phantom was composed of real bone structure and soft tissue equivalent material. Effective dose levels were evaluated only on head and neck organs because similar studies have shown that doses of other organs are negligible due to the maxillofacial tests [4].

Table 1. Cone Beam Computed Tomography examinations and exposure parameters in the predefined modes

Exposure parameter	Tube Voltage(KVP)	Tube current(mA)	Scan time (Sec)	Field of View(cm ²)	Voxel Size (μm)	DAP (mGy*cm ²)
Radiologic examination						
TMJ Standard	88	8	12.2	17.9*9.4	200	**
TMJ Low Dose	88	8	6.1	17.9*9.4	400	**
Dental Implant	88	8	12	5*5.7	200	489.5
Dental Endo	88	9	15	5*5.7	75	713
Sinus Standard	88	8	12	13*13	200	1540
Sinus Low Dose	88	8	6.05	13*13	400	771
Sinus ULD	88	4	3	13*13	400	217
Face STD	88	8	12	13*16	200	1856
Face LD	88	8	6	13*16	400	929
Face ULD	88	4	3.03	13*16	400	261

** : These items were not indicated by our CBCT system.

For every organ, the dose level was measured three times through imaging and TLD reading by Harshaw® Reader. ICRP version 103 tissue weighting factors were used for the calculation of effective dose as below:

$$H_T = W_R \sum_{T=0}^n D_T \quad E_T = \sum_{T=0}^n W_T H_T$$

Where H_T is the Equivalent Dose, D_T is Measured Dose, W_R is Radiation Weighting Factor, W_T is Tissue Weighting Factor, and E_T is the Effective Dose.

Calculation of Contrast -to -Noise Ratio (CNR) and Signal -to -Noise Ratio (SNR)

To evaluate the quality of the images, CNR and SNR were evaluated. For this purpose, the region of the tooth and soft tissue images were randomly used as the basis. The position of the region of interest (ROI) was determined by the radiologist and SNR and CNR were calculated through the following formula:

SNR= Mean intensity of ROI for dental tissue / standard deviation of dental tissue

CNR= (Mean intensity of ROI of dental tissue – Mean ROI of soft tissue)/standard deviation of soft tissue

Relative Effective Dose and SNR Reduction

Effective dose levels were evaluated only on the head and neck. For a better comparison of effective dose and SNR variations in different CBCT imaging techniques, relative dose reduction and relative SNR reduction was calculated through the following formula.

Relative dose reduction= ((dose in the desired mode- dose in the standard mode)/ dose in the standard mode)*100

Relative SNR reduction= ((SNR in the desired mode- SNR in the standard mode)/ SNR in the standard mode)*100

Statistical Analysis

Data analysis was performed by SPSS software version 16 (Chicago, IL, USA). The significance of data was analyzed using analysis of variance (ANOVA) and Tukey's post-hoc tests (P-value <0.05) and their normality was assessed by the Kolmogorov - Smirnov

test. Graphs were plotted by Microsoft Office Excel 2016.

Results

TLDs were inserted into various organs for dose assessment. Irradiation dose of right and left lens, parotid, and submandibular salivary glands as well as right and left thyroid lobes were measured simultaneously in every procedure including two TLDs for right and left thyroid lobes, two TLDs for right and left lens, two TLDs for right and left submandibular salivary glands, two TLDs for right and left parotid salivary glands, and two TLDs for right and left soft tissue of the neck. Most popular CBCT imaging procedures and their technical exposures were assessed for investigation of organs dose and each test was repeated three times. Some of the results are given in Table (2).

The dose of a specific organ varied significantly in different technical exposures of the same study. For instance, mean differences of thyroid dose in various technical exposures for face, sinus, TMJ, and dental imaging are indicated in Table 3. Mean differences were significant (P-Value< 0.05) in most procedures compared to the standard mode.

Dose levels of some anatomical structures on the right and left sides were different in some techniques. For instance, the mean absorbed dose of the right side of the lens, thyroid, submandibular, and parotid salivary glands was different compared to the left side (Figures 2&3). This may be due to the partial rotation of the tube.

For the calculation of effective dose level, organs average dose and ICRP version 103 tissue weighting factors were applied. Figure 4 shows the contribution of effective doses of different tissues for various CBCT imaging procedures.

In most cases, parotid glands, followed by facial muscles received higher doses than other structures. This may be due to their specific location in the radiation field. For this reason, submandibular salivary glands had the lowest radiation dose in most CBCT imaging procedures as shown in Figure 4.

Table 2. Organ dose in mGy: Mean ± standard deviation for different modalities.

Organ Modality	Thyroid	Submandibular Salivary gland	Neck	Soft Tissue	Parotid salivary Glands	Lens
Face STD	0.568 ± 0.05	3.166 ± 0.33	4.441 ± 0.19	3.743 ± 0.21	2.112 ± 0.18	
Face LD	0.289 ± 0.01	1.587 ± 0.11	2.268 ± 0.11	1.90 ± 0.83	1.035 ± 0.04	
Face ULD	0.157 ± 0.05	0.456 ± 0.05	0.640 ± 0.02	0.551 ± 0.02	0.356 ± 0.12	
Sinus STD	0.349 ± 0.04	0.670 ± 0.09	3.449 ± 0.37	3.926 ± 0.17	2.267 ± 0.12	
sinus LD	0.239 ± 0.05	0.3267 ± 0.04	1.675 ± 0.18	2.015 ± 0.16	1.074 ± 0.06	
sinus ULD	0.158 ± 0.03	0.145 ± 0.01	0.513 ± 0.08	0.609 ± 0.05	0.349 ± 0.15	
TMJ STD	0.696 ± 0.06	1.870 ± 0.28	10.54 ± 0.35	9.669 ± 0.39	2.294 ± 0.41	
TMJ LD	0.438 ± 0.02	0.879 ± 0.13	5.077 ± 0.33	4.497 ± 0.27	0.942 ± 0.52	
Dental Implant	0.264 ± 0.03	0.623 ± 0.08	1.806 ± 0.77	3.012 ± 0.28	0.324 ± 0.04	
Dental endo	0.326 ± 0.06	0.696 ± 0.07	1.214 ± 0.12	4.843 ± 0.73	0.537 ± 0.08	

Table 3. Mean differences, standard error, and significance values for thyroid (I: Standard mode, J: Low Dose or Ultra-Low Dose mode, *: significant (P-Value<0.05))

		Mean Difference (I-J)	Std. Error	Sig.	95% Confidence Interval	
					Lower Bound	Upper Bound
Face STD	Face LD	0.279*	0.028	0	0.187	0.371
	Face ULD	0.411*	0.027	0	0.319	0.503
Face LD	Face ULD	0.131*	0.027	0.001	0.039	0.223
Sinus STD	Sinus LD	0.110*	0.026	0.008	0.018	0.202
	Sinus ULD	0.191*	0.024	0	0.099	0.283
Sinus LD	Sinus ULD	0.080	0.027	0.129	0.011	0.172
TMJ STD	TMJ LD	0.258*	0.027	0	0.166	0.350

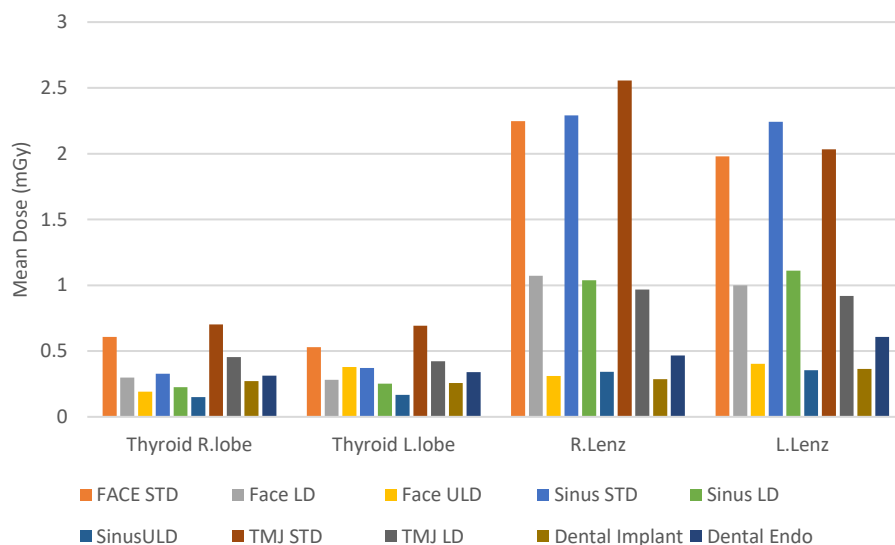


Figure 2. The mean absorbed dose level of right and left lens and thyroid lobes in different CBCT imaging procedures.

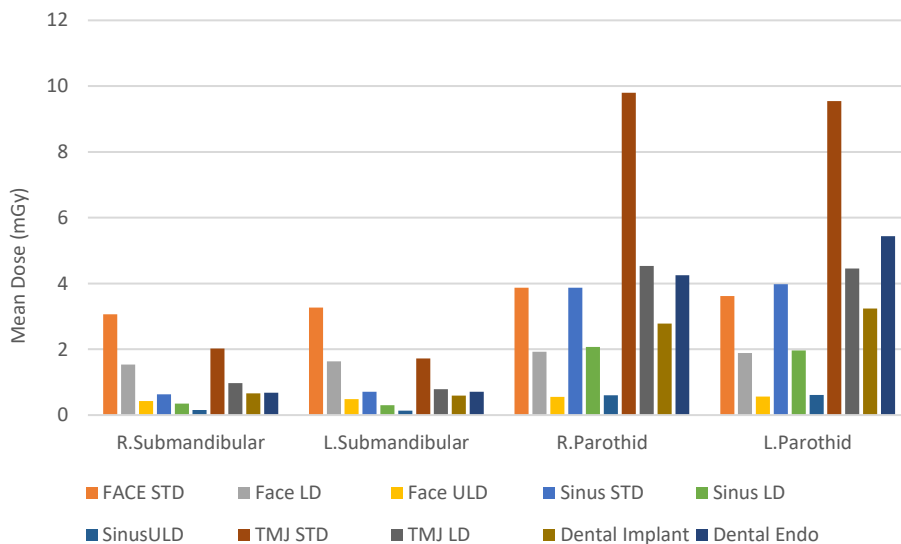


Figure 3. The mean absorbed dose level of the right and left parotid and submandibular salivary glands in different CBCT imaging procedures.

Total effective doses for every CBCT imaging technique were calculated through the formula mentioned in the Methodology Section. In most cases, the total effective dose for standard technique (STD) was at the highest level followed by low-dose (LD) and ultra-low-dose (ULD) techniques (Figure 5).

For assessment of image quality, SNR and CNR were calculated and the dose area product (DAP) parameter for every procedure was extracted from the CBCT system (Figure 6).

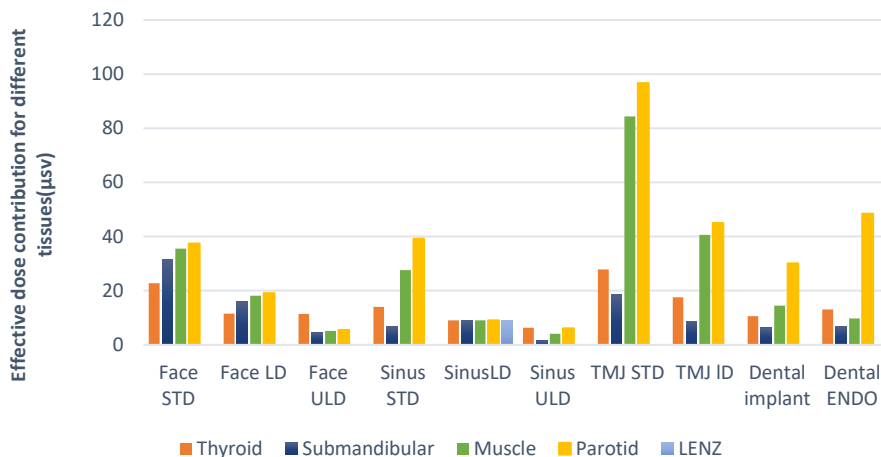


Figure 4. Contribution of effective doses in different tissues. STD: Standard, LD: Low-Dose, ULD: Ultra-Low Dose

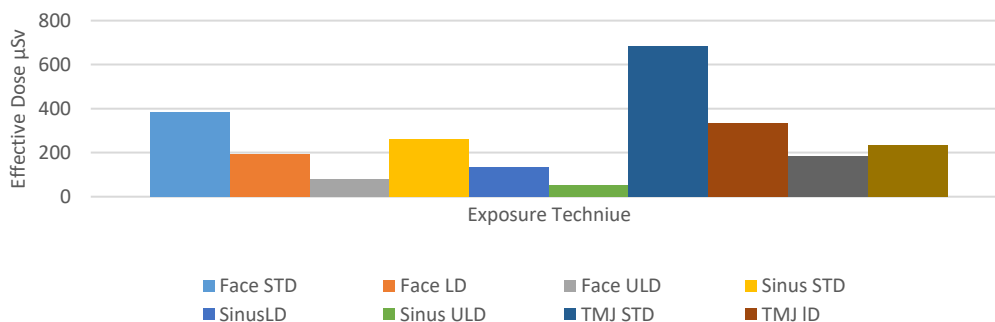


Figure 5. Total effective dose. STD: Standard, LD: Low-Dose, ULD: Ultra-Low Dose

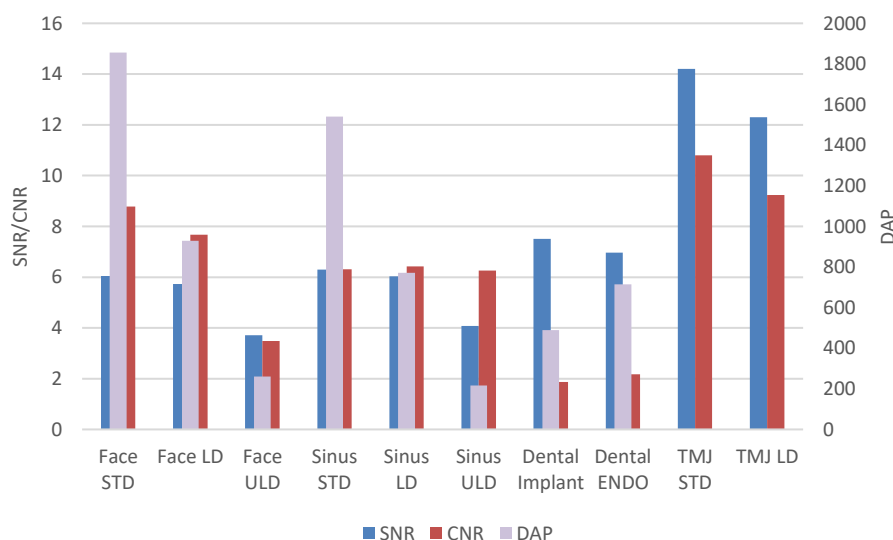


Figure 6. Signal-to-noise ratio (SNR), contrast-to-noise ratio (CNR) for different imaging procedures, DAP (mGy*cm²).

Table 4. Reduction of relative effective dose and relative reduction of SNR percentage

	Face STD	Face LD	Face ULD	Sinus STD	Sinus LD	Sinus ULD	TMJ STD	TMJ LD
Relative Effective Dose Reduction %	0	-49/2	-79	0	-48/3	-79/4	0	-50/8
Relative SNR Reduction %	0	-5/13	-38/5	0	-4/20	-7.93	0	-13/4

DAP parameter was at the highest level for the face standard exposure followed by paranasal sinus imaging in the standard mode. This is due to the higher exposure parameters and the large field of view (FOV) of these techniques. In our CBCT imaging, DAP was not calculated for TMJ imaging.

SNR parameter was at the highest level in the standard mode for every imaging procedure followed by low-dose and ultra-low-dose modes, respectively. This may have been influenced by higher exposure parameters in the standard mode.

The reduction of relative effective dose and relative reduction of SNR were analyzed, according to the formula given in the Methodology Section to compare different imaging techniques, in terms of dose and image quality (Table 4).

Discussion

In this study, we examined the effective dose for organs of the head and neck. In addition, we evaluated the image quality of different imaging modes through SNR and CNR assessment.

The patient's absorption dose is a function of exposure parameters and FOV, therefore an appropriate technique should be selected so that, the patient receives the minimum radiation dose while the resulting images have a suitable diagnostic quality[17, 18]. In our survey, FOV size was fixed for each CBCT technique for imaging of TMJ, dental implant, dental endo, and sinus structures (Table1).

Absorption dose in standard mode was at the highest level followed by low-dose and ultra-low-dose modes, respectively in our entire examinations (Table 2). This is due to higher values of time and tube current in the standard modes compared to low-dose and ultra-low-dose modes. The dose of organs changes in the same way. For example, the mean differences in thyroid dose were significant for low-dose and ultra-low-dose modes compared to the standard mode (Table 3). These findings are consistent with the results of similar studies [17-20].

The dose level on both sides of the head and neck for different organs was evaluated in the current survey. Irradiation doses of right and left lens, parotid, and submandibular salivary glands, as well as right and left thyroid lobes, were different in some techniques as shown in Figs. 2&3. For example, in the right TMJ and face imaging with standard protocol, the dose of the right lens and parotid was greater than the opposite lens (Figs. 2&3). This is due to partial tube rotation during exposure. In both examinations, the tube had 270 degrees of arch rotation.

In our survey for most of the studied imaging procedures, the highest effective dose contribution was related to the parotid salivary glands followed by the muscles, thyroid and then, submandibular salivary glands (Figure 4). This can be attributed to the anatomical extent of these organs and their position in the radiation field, which is consistent with the results of similar studies [4, 21, 22].

In CBCT imaging of paranasal sinuses (standard protocol), the parotid salivary gland had the most effective dose contribution and the submandibular salivary gland had the lowest contribution (Figure 4). This can be due to their size and situation. In CBCT imaging of paranasal sinuses (low-dose protocol), all the studied organs had a similar contribution of effective dose level (Figure 4), although they had various dose levels (Table 2), which may be due to the various applied tissue weighting factors.

Figure 5 shows the total effective dose for the most common CBCT examinations in three modes (standard, low-dose, and ultra-low-dose). The highest effective dose was related to TMJ in standard mode followed by face standard mode and TMJ at low-dose mode imaging. Their large FOV, higher mA, and exposure time (Table 1) caused an increase in the patient's dose, which is compatible with similar studies [4, 18, 21, 23].

Spatial resolution and image quality in CBCT imaging are determined by FOV size, 2D detector, 3D reconstruction process, and patient's movement during scanning. Image quality is an important issue in CBCT, because image details are crucial for better diagnosis of dental and maxillofacial pathologies[23, 24].

In our survey, for every studied procedure, the standard protocol had the highest SNR and CNR values due to their high exposure setting (mA, KVP, and acquisition time) compared to LD and ULD techniques (Figure 6). Increasing the time and mA leads to an increase in the intensity of photons and noise reduction, resulting in SNR improvement. CNR is also influenced by the background noise and density differences. Thus, the increase of exposure time and mA will result in CNR improvement (Figure 6).

DAP parameter was at the highest level for the face standard exposure followed by paranasal sinus imaging in standard mode. This is due to the higher exposure parameters and large FOV in these techniques. In our CBCT imaging, DAP was not calculated for TMJ imaging (Figure6).

In CBCT imaging of paranasal sinuses, among the three modes of standard, low-dose, and ultra-low-dose, DAP and CNR values were almost close together (Figure 6), but due to the difference in dose levels, low-

dose and ultra-low dose protocols are suggested for imaging (Table 2).

Table 4, shows the results regarding the reduction of relative effective dose and relative reduction of SNR to compare different imaging techniques in terms of dose and image quality. When a low-dose mode was chosen, the patient's dose was reduced in the face, sinus, and TMJ imaging by 49.2%, 48.3%, and 50.8%, respectively while the percentage of relative SNR reduction was obtained as 5.13, 4.2, and 13.4, respectively. A serious dose reduction was obtained using low-dose mode, while there is no significant decrease in the SNR rate.

Also, according to Table 4, the selection of ultra-low-dose mode induced a significant decrease in the dose and SNR rate.

Thus, the use of low and very low-dose modes should be a priority for cases where sufficient diagnostic information is obtained by these modes.

According to Table 1, reduction of exposure time, milliamperes, and FOV induce to patient's dose reduction. The radiographer must select these factors intelligently concerning the patient's anatomy to optimize the dose. At the same time, image quality should be considered. Access to various CBCT units was our limitation for this study. For further research, it is recommended that this study be performed on other CBCT systems.

Conclusion

When low-dose and ultra-low-dose modes are selected, the patient's dose will be severely reduced in most CBCT procedures while CNR and SNR factors show less reduction and the acquired images have sufficient quality for many diagnostic purposes.

Acknowledgment

The authors appreciate all those who contributed to this project. This project was funded by the Student Research Committee of Mashhad University of Medical Sciences.

References

- Farman, A.G. and W.C. Scarfe. The basics of maxillofacial cone-beam computed tomography. in *Seminars in Orthodontics*. 2009. Elsevier.
- Alamri HM, Sadrameli M, Alshalhoob MA, Alshehri MA. Applications of CBCT in dental practice: a review of the literature. *General dentistry*. 2012 Sep 1;60(5):390-400.
- Dawood A, Patel S, Brown J. Cone beam CT in dental practice. *British dental journal*. 2009 Jul;207(1):23-8.
- Loubele M, Bogaerts R, Van Dijck E, Pauwels R, Vanheusden S, Suetens P, et al. Comparison between effective radiation dose of CBCT and MSCT scanners for dentomaxillofacial applications. *European journal of radiology*. 2009 Sep 1;71(3):461-8.
- White SC, Pharoah MJ. The evolution and application of dental maxillofacial imaging modalities. *Dental Clinics of North America*. 2008 Oct 1;52(4):689-705.
- C Cangul S, Adiguzel O. Cone-beam three-dimensional dental volumetric tomography in dental practice. *International Dental Research*. 2017 Dec 31;7(3):62-70.
- Agrawal JM, Agrawal MS, Nanjannawar LG, Parushetti AD. CBCT in orthodontics: the wave of future. *The journal of contemporary dental practice*. 2013 Jan 1;14(1):153.
- Galiccia JC, Kawilarang J, Tawil PZ. Clinical endodontic applications of cone beam-computed tomography in modern dental practice. *Open Journal of Stomatology*. 2017 Jul 17;7(7):314-26.
- Carter JB, Stone JD, Clark RS, Mercer JE. Applications of cone-beam computed tomography in oral and maxillofacial surgery: an overview of published indications and clinical usage in United States academic centers and oral and maxillofacial surgery practices. *Journal of Oral and Maxillofacial Surgery*. 2016 Apr 1;74(4):668-79.
- Ludlow JB, Ivanovic M. Comparative dosimetry of dental CBCT devices and 64-slice CT for oral and maxillofacial radiology. *Oral Surgery, Oral Medicine, Oral Pathology, Oral Radiology, and Endodontology*. 2008 Jul 1;106(1):106-14.
- Li G. Patient radiation dose and protection from cone-beam computed tomography. *Imaging science in dentistry*. 2013 Jun 1;43(2):63-9.
- Ludlow JB, Davies-Ludlow LE, Brooks SL, Howerton WB. Dosimetry of 3 CBCT devices for oral and maxillofacial radiology: CB Mercuray, NewTom 3G and i-CAT. *Dentomaxillofacial radiology*. 2006 Jul;35(4):219-26.
- Roberts JA, Drage NA, Davies J, Thomas DW. Effective dose from cone beam CT examinations in dentistry. *The British journal of radiology*. 2009 Jan;82(973):35-40.
- Mah JK, Danforth RA, Bumann A, Hatcher D. Radiation absorbed in maxillofacial imaging with a new dental computed tomography device. *Oral Surgery, Oral Medicine, Oral Pathology, Oral Radiology, and Endodontology*. 2003 Oct 1;96(4):508-13.
- Soares MR, Santos WS, Neves LP, Perini AP, Batista WO, Belinato W, et al. Dose estimate for cone beam CT equipment protocols using Monte Carlo simulation in computational adult anthropomorphic phantoms. *Radiation Physics and Chemistry*. 2019 Feb 1;155:252-9.
- Attaia D, Ting S, Johnson B, Masoud MI, Friedland B, El Fotouh MA, et al. Dose reduction in head and neck organs through shielding and application of different scanning parameters in cone beam computed tomography: an effective dose study using an adult male anthropomorphic phantom. *Oral Surgery, Oral Medicine, Oral Pathology and Oral Radiology*. 2020 Jul 1;130(1):101-9.
- Katz F. Reducing CBCT radiation dose and maintaining image quality for reliable cephalometric measurements—proof of concept (Doctoral dissertation).
- Nascimento HA, Andrade ME, Frazão MA, Nascimento EH, Ramos-Perez FM, Freitas DQ. Dosimetry in CBCT with different protocols: emphasis on small FOVs including exams for TMJ. *Brazilian Dental Journal*. 2017 Jul;28:511-6.

19. Andrade ME, Khoury HJ, Nascimento Neto JB, Kramer R. Dosimetric evaluation of dental implant planning examinations with cone-beam computed tomography. *Radiation protection dosimetry*. 2014 Jan 1;158(2):175-80.
20. Feragalli B, Rampado O, Abate C, Macrì M, Festa F, Stromei F, et al. Cone beam computed tomography for dental and maxillofacial imaging: technique improvement and low-dose protocols. *La radiologia medica*. 2017 Aug;122(8):581-8.
21. Qu X, Li G, Zhang Z, Ma X. Thyroid shields for radiation dose reduction during cone beam computed tomography scanning for different oral and maxillofacial regions. *European journal of radiology*. 2012 Mar 1;81(3):e376-80.
22. Almuqrin AH, Tamam N, Abdelrazig A, Elnour A, Sulieman A. Organ dose and radiogenic risk in dental cone-beam computed tomography examinations. *Radiation Physics and Chemistry*. 2020 Nov 1;176:108971.
23. Pauwels R. Cone beam CT for dental and maxillofacial imaging: dose matters. *Radiation protection dosimetry*. 2015 Jul 1;165(1-4):156-61.
24. Brüllmann D, Schulze RK. Spatial resolution in CBCT machines for dental/maxillofacial applications—what do we know today?. *Dentomaxillofacial Radiology*. 2015 Jan;44(1):20140204.